Detailed presentation of the results obtained in the research project K-129037

In the first segment of the research we prepared an extended library of antiproliferative chalcone-cinchona hybrids including quinine (**1**, **1***, **3*** and **5***) and quinidine (**2**, **2***, **4*** and **6***) alkaloid core. The novel hybrids tethered by 1,2,3-trizole linkers with 1,4-substitution- and 1,5-patterns were accessed by optimised copper- and ruthenium-catalized azide-alkyne [2+3] annullations of didehydroquinine- and quinidine with *ortho*-and *para* azidosubstituted chalcones [1]. The cycloadditions were accompanied by transition-metal catalysed partial or full epimerisation at C9 position of the cinchona residue leadig to chelate-stabilized isomers (**1***–**6***). This process is assumed to be promoted by reversible metal coordination to the quinoline N1 atom increasing the acidity of Pos.9.

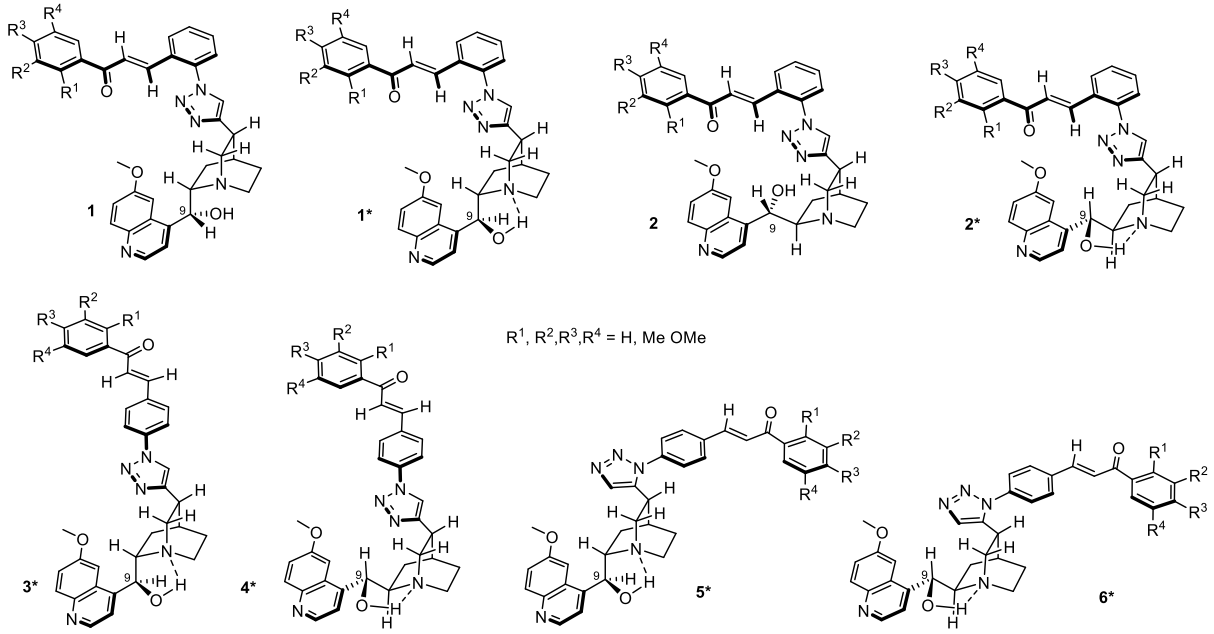

Figure 1.

The hybrids were subjected to in vitro tests on PANC-1, COLO-205, A-2058 és EBC1 cell lines and exhibited antiproliferative activity in low micromolar concentrations. The derivatives with 3,4,5-trimethoxy substituted chalcone moiety (R^1=H, R^2=R^3=R^4=OMe) were identified as particularly active agents with activity in low micomolar- or submicromolar concentration. In order to get preliminary information on the mechanism of their action at cellular level, cell-cycle analyses were performed using the most efficient epiquinidine-based hybrid compraising a 1,5-disubstituted triazole linker and a substantially less active counterpart with 1,4-disubstituted triazole linker as suitably selected models. In PANC-1 cells the active one induced a significant increase in the subG1 phase and also in the percentages of S and G2/M [1].

We have also prepared chalcone hybrids containing ferrocenoylamino group in pos. 9 tethered by 1,4-disubstituted triazole-linker (**7**–**9**: Figure 2). Using an array of well-documented ruthenium-based catalytic systems and conditions, a number of experiments were directed to construct a 1,5-disubstituted triazole linker within this molecular architecture, however all of these attempts failed so far. The hybrids derived from successful copper-catalysed triazole anullation were evaluated on further cells including HeLa (cervival cancer), A2780 (ovarian cancer) and triple negative MDA-MB-231 (brest cancer) and displayed substantial activity at low and submicromolar concentrations. It is of note that compound **8d** (R^1=H, R^2=R^3=R^4=OMe) was identified as far the most potent antiproliferative agent chracterized e.g. by IC_{50} value of 386 nM measured on A2780 cells. On the basis of the results novel structure-activity relationships were established pointing to the essential contribution of ferrocenoylamino group at pos. 9 of the cinchina units to the antiproliferative effect, as **10**, the benzoyl counterpart of **8d** proved to be markedly less active than the highly potent ferrocene analogue. The

preparation of the manuscript reporting on the synthesis and antiproliferative effect of this group of hybrids is in progress [2].

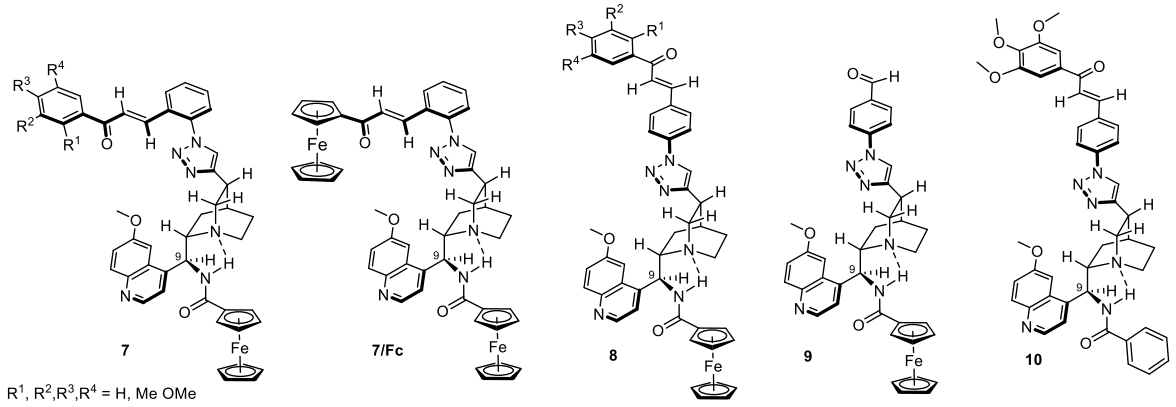

Figure 2.

Searching for highly efficient antiproliferative chalcone hybrids we aimed to design antitumor hybrid compounds based on an inhibitor of ataxia-telangiectasia and Rad3-related protein (ATR)-dependent signaling, protoapigenone, and a pro-oxidant ferrocene or chalcone fragment. Four further triazole-coupled hybrids (**12a**–**d**) were prepared exploiting hypervalent iodine-mediated oxidative coupling of protoflavone with propargylalcohole followed by CuAAc coupling (Scheme 1).

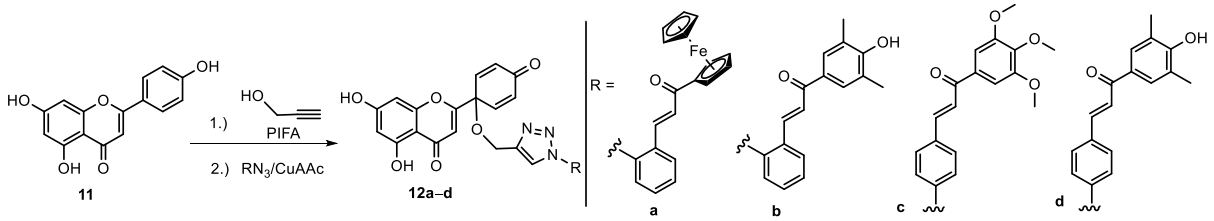

Scheme 1

The compounds were found to be cytotoxic against human breast cancer cell lines in vitro, showing IC_{50} values in the sub-micromolar range. The nature of interactions between relevant fragments of the hybrids was evaluated by the Chou–Talalay method. Experimental combination treatment with the fragments showed additive effects or slight/moderate synergism, while strong synergism was observed when the fragments were virtually combined into their hybrids, suggesting a relevant pharmacological benefit of the coupling. All hybrids were strong inhibitors of the ATR-mediated activation of Chk1, and they interfered with the redox balance of the cells leading to mitochondrial membrane depolarization. Additionally, they induced late apoptosis and primary necrosis in MDA-MB-231 and MCF-7 breast cancer cells, respectively. Our results demonstrate that coupling the ATR-dependent signaling inhibitor protoflavone with a pro-oxidant chalcone dramatically increases the antitumor activity compared with either fragment alone [3].

By inclusion into chalcone hybrids we aimed to enhance the anti-cancer efficacy of erlotinib and some representative chalcones which displayed as single agents by their incorporation into hybrids with potential multitarget character containing acetylenic and triazole linkers between these pharmacophoric molecular fragments [4]. Thus, a series of novel hybrids were accessed by copper(I)-catalyzed azide-alkyne [2+3] cycloadditions and Sonogashira coupling reactions followed by standard Claisen-Smith condensation. Since tumor heterogeneity and consequently drug resistance in HNSCC represent a great unmet medical need for more efficient drug therapies, the novel hybrids were tested in three HNSCC cell lines Fadu, Detroit 562 and SCC-25. Investigation of the hybrids was focused on such features of their anti-cancer potential, which may be manifested in their pronounced ability to overcome resistance in these cancers. Screening assay, followed by time- and dose-dependent cell viability measurements demonstrated that most prominent hybrids (**13** and **14**) have efficacy superior to their molecular fragments Erlotinib and a reference chalcone also revealing specific structure-activity relationships. It is of pronounced importance that molecular hybridisation showed very strong synergism of the fragments in the low-micromolar range in all of the three HNSCC cell lines as demonstrated by their superior activity compared to combined therapy (Figure 3). After 72 h treatment

followed by 72 h incubation time hybrid **13** resulted in the total eradication of all the investigated cancer cells at 2.5 µM, while **14** also proved to be markedly efficient against Fadu and Detroit-562 cells. Experiments focusing on mechanism of actions indicated that the enhanced efficacy of the most potent hybrids are independent from the canonical molecular targets of their molecular fragments pointing to the need of further explorations directed to disclose the cause of their prominent efficacy allowing rational design of more potent members of this highly promising hybrid family [4].

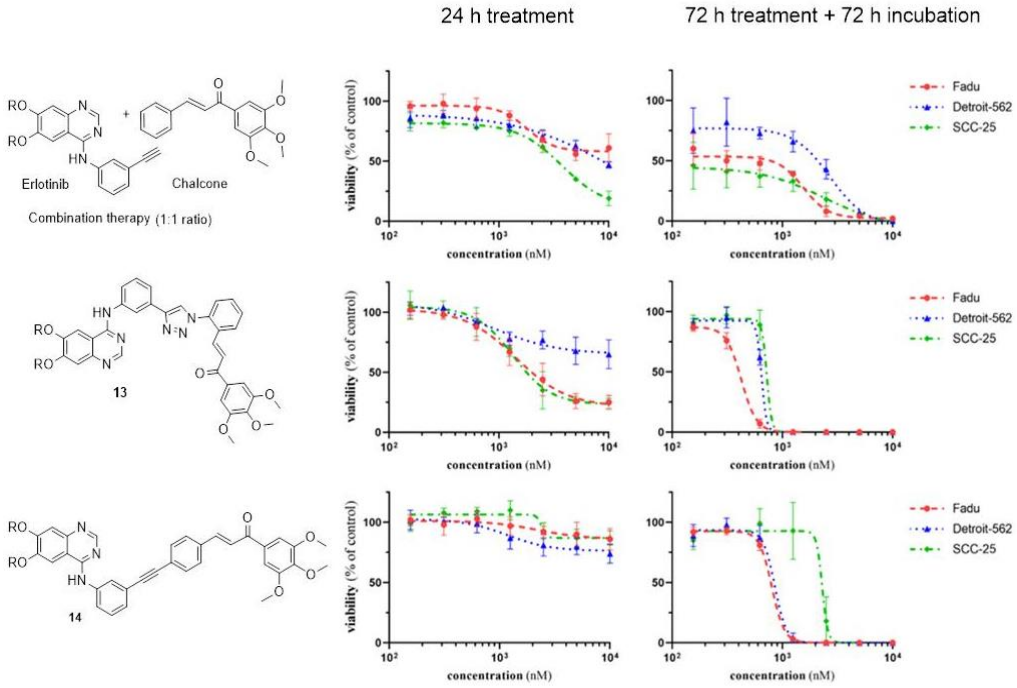

Figure 3.

A series of novel 1,2,4-thiadiazoles bearing Erlotinib, phenylethynyl, ferrocenyl, and/or ferrocenethynyl moieties (types **16** and **17**: Scheme 2) were also synthesized and characterized by NMR, IR and mass spectroscopies [5]. The solid-phase structures were determined by single-crystal X-ray diffraction. Partial isomerisation of bis(erlotinib)-1,2,4-thiadiazole into its 1,3,4-thiadiazole isomer (**17** →**18**), leading to the isolation of a 3:2 isomer mixture, was observed and a modelling-supported mechanism involving a cooperative catalytic effect of Pd- and Cu species for isomerisation was suggested [5]. The *in vitro* cytostatic effect and the long-term cytotoxicity of these thiadiazole-hybrids, as well as that of Erlotinib, 3,5-dichloro-1,2,4-thiadiazole and 3,5-diiodo-1,2,4-thiadiazole were investigated against A2058 human melanoma, HepG2 human hepatocellular carcinoma, U87 human glioma, A431 human epidermoid carcinoma, and PC-3 human prostatic adenocarcinoma cell lines. Interestingly, Erlotinib did not exhibit a significant cytostatic effect against these cancer cell lines. 1,2,4-Thiadiazole hybrids bearing one Erlotinib moiety or both an iodine and a ferrocenethynyl group, as well as 3,5-diiodo-1,2,4-thiadiazole demonstrated marked cytostatic effect. Among the synthesized 1,2,4-thiadiazole hybrids, the isomer mixture of bis-erlotinib substituted 1,2,4- and 1,3,4-thiadiazoles showed the most potent activity [5]. Very recently, starting from the commercially available 2,5-dibromo-1,3,4-thiadiazole **19** isomer **18** was also prepared in pure form (Scheme 2) and - as soon as possible - will be subjected to biological tests to assess the relative efficiency of the components of the 3:2 mixture.

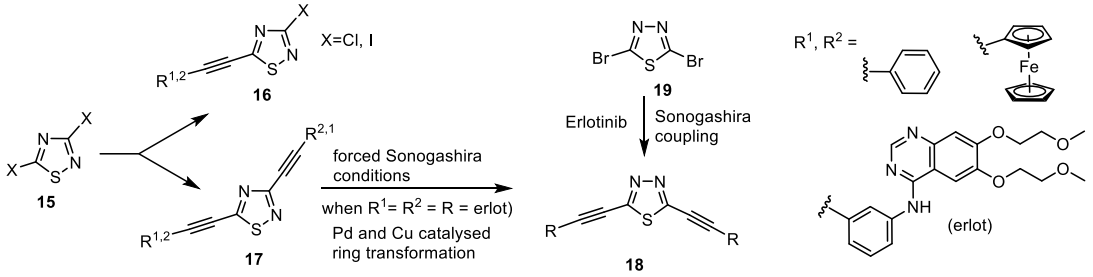

Scheme 2.

Use of a Pictet-Spengler reaction of tryptamine and l-tryptophan methyl ester (**20** and **21**: Scheme 3) and subsequent reduction of the nitro group followed by further cyclocondensation with aryl aldehydes and formyl–substituted carboxylic acids, including ferrocene-based components, furnished a series of diastereomeric 6-aryl-substituted 5,6,8,9,14,14b-hexahydroindolo[2′,3′:3,4]pyrido[1-*c*]-quinazolines and 5,5b,17,18-tetrahydroindolo[2′,3′:3,4]pyrido[1,2-*c*]isoindolo[2,1-*a*]quinazolin-11-(15b*H*)-ones with the elements of central-, planar and conformational chirality (**22**-**25**: Scheme 3) [6]. The relative configuration and the conformations of the novel polycyclic indole derivatives were determined by ^{1}H- and ^{13}C-NMR methods supplemented by comparative DFT analysis of the possible diastereomers. The structure of one of the pentacyclic methyl esters with defined absolute configuration "*S*" was also confirmed by single crystal X-ray diffraction measurement. Accounting for the characteristic substituent-dependent diastereoselective formation of the products multistep mechanisms were proposed on the basis of the results of DFT modeling. In vitro cytotoxic assays of the products revealed moderate-to-significant antiproliferative effects against PANC-1-, COLO-205-, A-2058 and EBC-1 cell lines that proved to be highly dependent on the stereostructure and on the substitution pattern of the pending aryl substituent. Compound **22/T** carrying 3-trifluoromethylphenyl substituent was identified as far the most potent antiprolifertaive agent displaying activity in low micromolar concentrations even in racemic form [6].

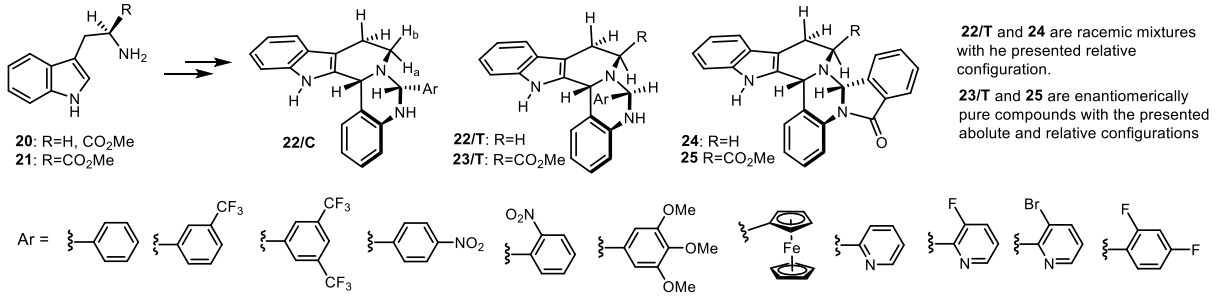

Scheme 3.

Prompted by the highly promising potency of the aforementioned racemate, by means of multistep reaction sequences exploring two enantiomeric tryptophanoles (**26**) as precursors we performed the synthesis and NMR structural elucidation of the enantimeric pairs of hydroxymethyl-substituted pentacycles type **27** (Scheme 4) suitable to further functionalisations, The biological evaluation of the enantiomers is in progress. Upon completion and evaluation of the *in vitro* cell viability assays and functional studies, the results of the chemistry and biology of these compounds will be reported in a paper which will be submitted to a high-standard journal.

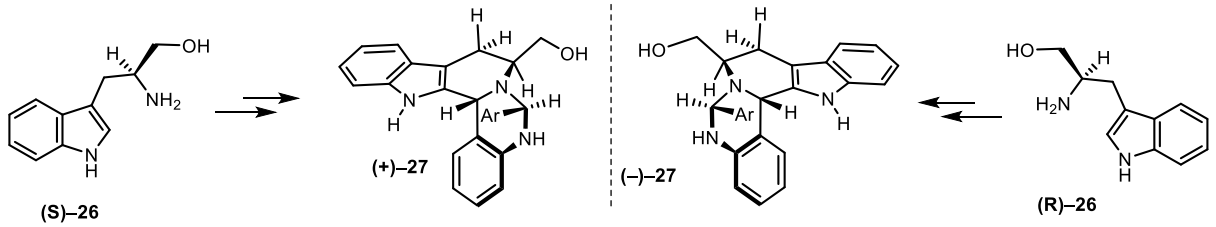

Scheme 4.

We conducted a detailed synthetic and mechanistic study on the complex transformations of 4,5-dibromo-pyridazin-3(2*H*)-one (**28**), an apparently simple heterocyclic bifunctional building block explorable in pharmaceutical chemistry, with ferrocene-containing boronate components under a variety of Suzuki-Miyaura (SM) conditions [7]. While double coupling of **28** with phenylboronic acid provided the expected product **29** in excellent yields, under the same conditions the ferrocene-boronate-mediated Suzuki-Miyaura reactions run in water-containing solvent mixtures were accompanied by hydrodebromination processes affording bis- and isomer monoferrocenyl-substituted products **30**–**32** along with ferrocene resulted from the fission of C-B bond (Scheme 5). By control experiments and theoretical modeling studies we disclosed that the hydrodebromination processes are specifically promoted by the primarily introduced ferrocenyl group in the appropriate

bromopyridazinone intermediate or by a ferrocene-containing species present in the reaction mixture [7].

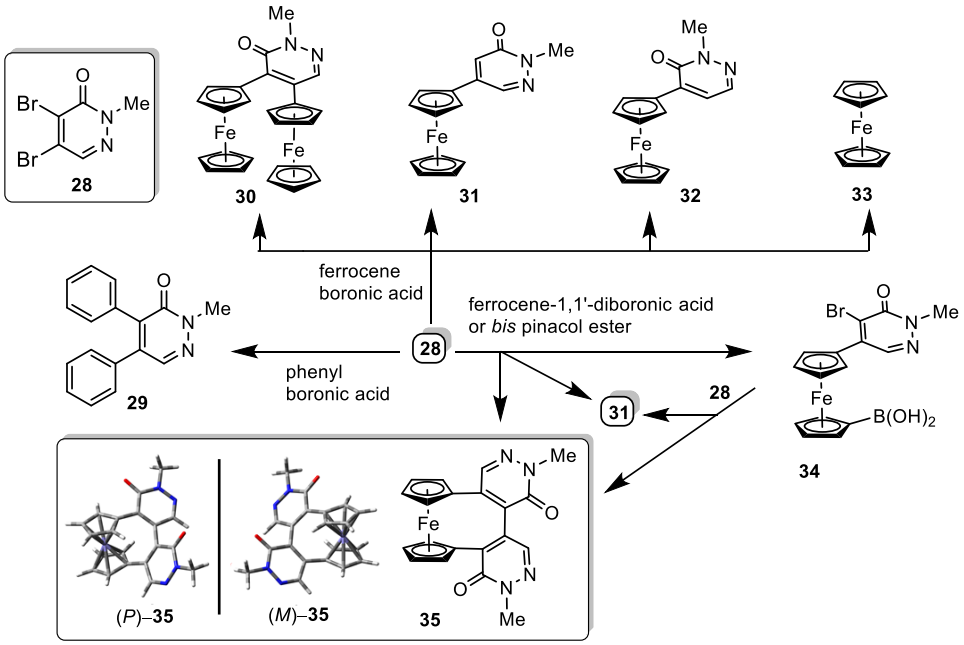

Scheme 5.

The catalyst-dependent experimental product distributions were found to be correlated with the relative energetics of the critical elementary steps and regioisomer key intermediates of the competitive polar and radical multistep reaction pathways. We also recognized and rationalized a bridge-forming annulation that assembled the first representative of a novel class of heterocyclic ferrocenophanes featuring asymmetric constitution with rigid helical chiral conformation (**35**). Even in racemic form as isolated [(*P*)–**35**) and (*M*)–**35**)], this ferrocenophane demonstrated antiproliferative activity in low micromolar concentration against two human malignant cell lines (A431 and HepG2). Pointing to the essential role of the organometallic moiety in triggering cytotoxicity, **29** was identified as an inactive organic reference, whereas its differocenyl counterpart (**30**) displayed substantial cell-line selective effect under *in vitro* conditions [7]. The family of the ferrocene-containing anticancer pyridazinones we presented in Ref. 7 can be extended by the replacement of the *N*-methyl group for an array of substituents including privileged building blocks found e.g. in documented therapeutic agents.

In the course of the whole project period along with 9 reference imipridones including ONC212 disclosed in prior-art, we synthetized 140 novel imipridones type **36** (Figure 4) and filed in our international patent application WO2022029459A1 (*its IP status and results so far*: patent application filed and granted in 2020, PCT application filed and granted in 2021, national patents currently filed across more than 35 countries) [8]. Our invention relates to the development of novel imipridones with substituent patterns implicating substituents X, Y and Z undisclosed in the patents and other publications of our competitors. The compounds are applicable for use in treating human tumorous diseases such as pancreatic cancer, brest cancer, lung cancer, colorectal cancer, gliomas, melanoma prostate cancer as well as head- and neck cancers. The invention further relates to single enantiomers and racemic mixtures when the fragment $ZCH_2CH(X)$- with a stereogenic center attached to the skeletal N4-atom.

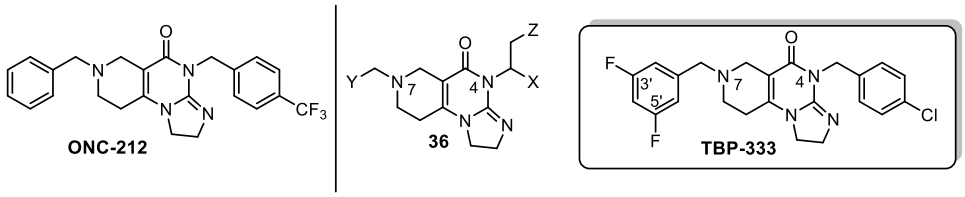

Figure 4.

The emblematic ONC212 (Figure 4) identified as the most potent second-generation imipridone patented by our competitors was selected to be used as a positive reference of which efficacy was compared to that of our filed molecules which were tested on a wide array of human malignant cell lines of different tissue origin (PC4, LNCaP, PANC-1, BxPC3, MiaPaCa2, A549, HCC827, H1993, H520, MDA-MB-453, MDA-MB-231, EBC-1, H2228, SCC-25, Fadu, Detroit-562). The antiproliferative activity of the most potent drug candidates can be characterised by IC_{50} values of 1-5 nM. In this context TBP333 (Figure 4) identified as the most potent drug candidate in our invention exhibited substantially higher *in vitro* efficacy on all of the investigated cancer cells compared to ONC212 as spectacularly exemplified by selected dose-response curves outlined in Figure 5.

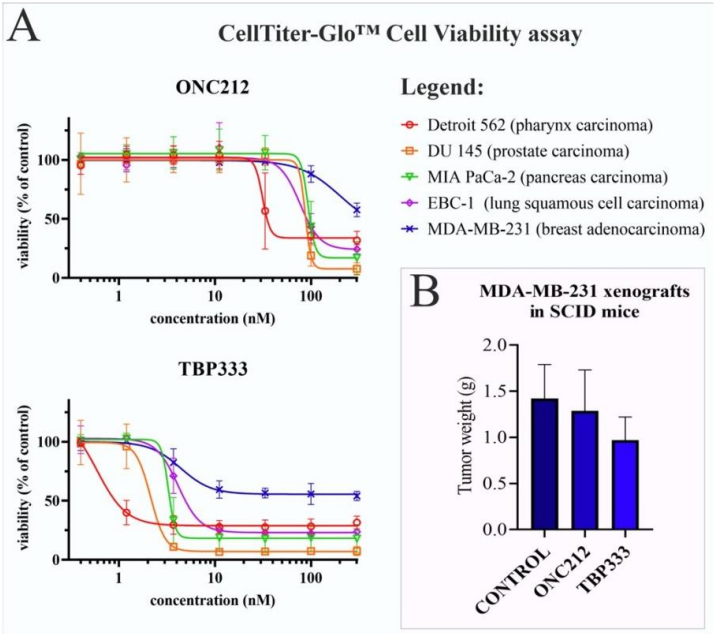

Figure 5.

The efficient doses at low nanomolar range found for TBP333 are typically lower by 1-3 orders of magnitude relative to those produced by ONC212. To our best knowledge, in terms of efficient doses and IC_{50} values, TBP333 is the most potent member of the anticancer imipridone family identified so far. Moreover, featuring a low-level toxicity comparable to that of ONC212, TBP333 demonstrated a significantly stronger antitumor effect on MDA-MB-231 human triple-negative breast cancer xenografts in immune-suppressed mice compared to ONC212 (Figure 5).

Constituting an integrated part of our invention we also disclosed special imipridone-related structure-activity relationships establishing that introduction of 3',5'-difluorobenzyl substituent in position 7 dramatically increases the anticancer activity. Meantime, this activity-enhancement has been proven to be mainly associated with the formation of a well-defined complex of TBP333 with mitochondrial ClpP, the main cellular target of imipridones as evidenced by x-ray diffraction analysis in the frame of an international research cooperation proposed and initiated by the leader of a team

(Professor Walid Houry, Toronto University) having close personnel, scientific and innovative connections with our competitors.

Despite the promising anti-proliferative and pro-apoptotic effects of ClpP-activators, the resistance of cancer cells to the treatment seems to be a persistent problem. In this regard, several studies identified imipridones as effective cytotoxic agents in micro- or nanomolar concentrations, however the measured dose-response curves showed that approximately 10-50% of the cells survived the treatment, even at higher imipridone concentrations and after prolonged exposure times. To address the problem associated with incomplete eradication of tumor cells we have undertook the synthesis and evaluation of hybrids containing redox active ferrocene units tethered by electron-transmitter triazole- or alkyne linker to the imipridone scaffold [9]. This choice of strategy was based on the documented fact that imipridones cause a structural damage of mitochondria and elevated levels of mitochondrial ROS, thus we expected a synergistic cross-talk between the ROS-mediated effect of ferrocene-containing fragment(s) and the imipridone-induced TRAIL- and ClpP activation that might substantially increase the cytotoxicity of the hybrid compounds. Thus, by means of combined application of synthetic strategies based on diazotation-azidation sequence, orthogonal CuAAc-and RuAAC procedures along with Sonogashira protocols we prepared 26 novel imipridone hybrids and identified propargylamine **37c** with 4-ferrocenyltriazol-1-yl substituent in the para position on the *N*-7 benzyl group of the imipridone core , which unlike first-generation imipridone ONC201, is capable of completely eradicating the investigated tumour cells at around 10 micromolar concentrations (Figure 6) [9].

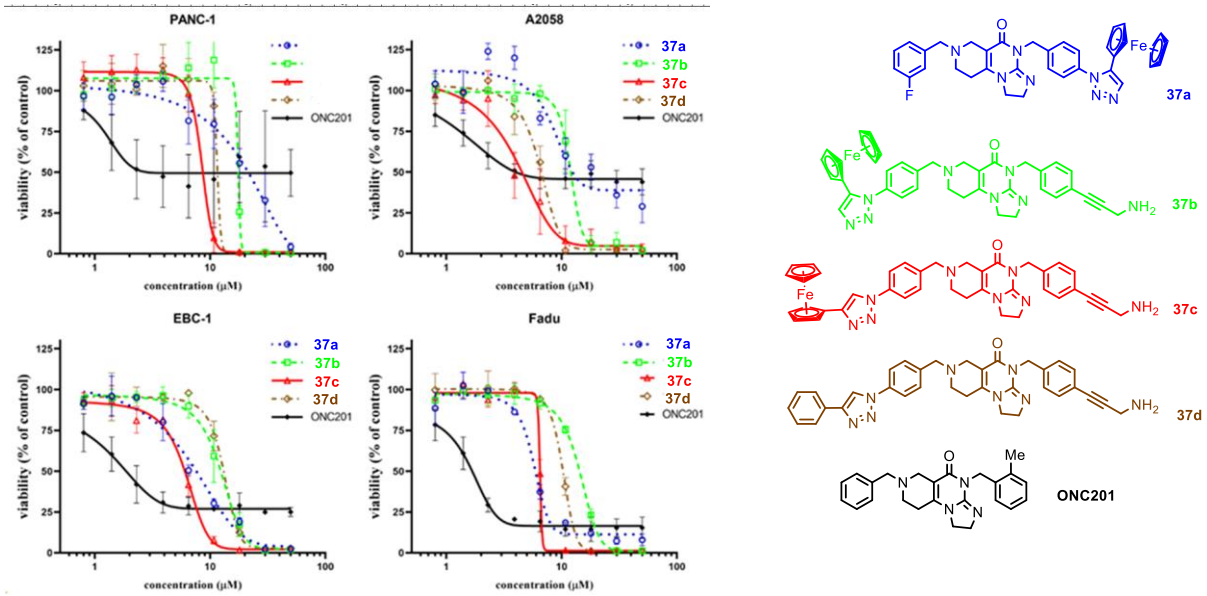

Figure 6.

Aiming at decreasing the efficient dose of type **37** hybrids with retained potency to completely eradicate the cancer cells, we synthetised and tested furter 42 analogues by changing the substitution pattern on the terminal benzyl groups [10]. Finally, *meta*-positioned *N*-methylpropargylamines **37e** and **37f** of enhanced basicity were identified as the most potent antiproliferative agents featuring complete eradication of PANC-1 and Fadu cells and lower efficient doses compared to ONC201. Mechanistic studies disclosed that ferrocene derivative **37f** triggers apoptosis, while neither **37e** nor **37f** was found to be active on ClpP-KO cells warranting further funcional studies directed to identification of the main cellular target. Thus, the submission of the manuscript reporting on the synthetic and biological results [10] needs to be postponed until the completion of the biological part of this research.

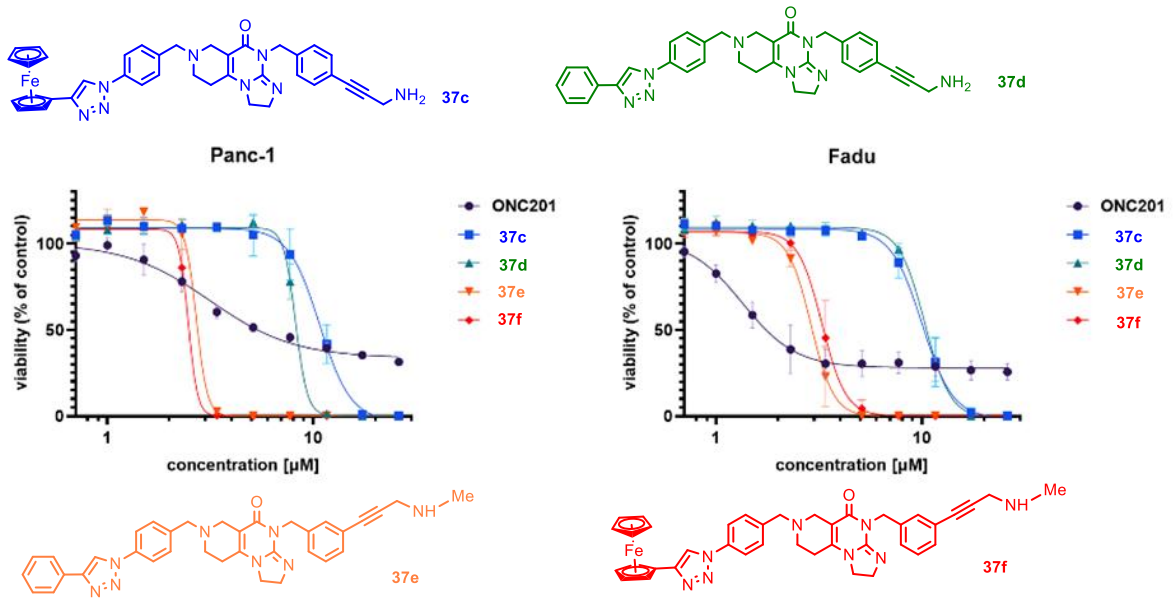

Figure 7.

With the structure activity relationships in hands, collected so far including the canceled activity of compounds **37** on ClpP, we aimed to extend the chemical space of active imipridones with retained ClpP binding affinity and suitably positioned functional groups that allow molecular hybridization to other pharmacophores. Thus, exploring a multistep pathway proceeding *via* propargylation and subsequent Sonogashira coupling-along with an *N*-protection-deprotection sequence we constructed imipridone hybrids embedding arylamines tethered to optimally substituted imipridone core *via* alkyne-containing linker attached to a stereogenic center of *R*-chirality (**38a-c:** Scheme 2)**.** These products feature benzyl-substitution pattern identical to that of TBP333. Alkynes of types **38** were evaluated for their *in vitro* antiproliferative activity on PANC-1 and head and neck cancer cell lines (Fadu, Detroit, SCC-25) and were found to be highly active in the cell viability assays featuring efficient doses at low nM concentrations comparable to those measured for TBP333. Notably, **38c** displayed even somewhat stronger effect on PANC-1 cells than TBP333, but samples suitable for x-ray diffraction could only be obtained by co-crystallization of **38b** and purified ClpP. The co-crystallized complexes of TBP333 and **38b** were analyzed by x-ray diffraction in the laboratory of University of Toronto. Our Canadian partner established that the complex of TBP333 demonstrates an exceptional stability due to a network of interatomic interactions involving the 3,5-difluorobenzyl group ideally fitting in the binding pocket of the protease. More importantly, in comparative experiments both TBP 333 and **38b** showed substantial binding affinity to ClpP. The imipridone core of the latter molecule was found to be embedded in the H-region with orientation highly similar to that of ClpP-binded TBP333, carrying the alkyne-containing side chain with decreased flexibility protruding from the surface of the protease complex (Scheme 6). Encouraged by these results we envisage the synthesis, structural- and biological evaluation of further alkyne tethered derivatives. The results of this research, being currently in progress in the frame of international cooperation, will be published in a high-standard journal with D1 rank.

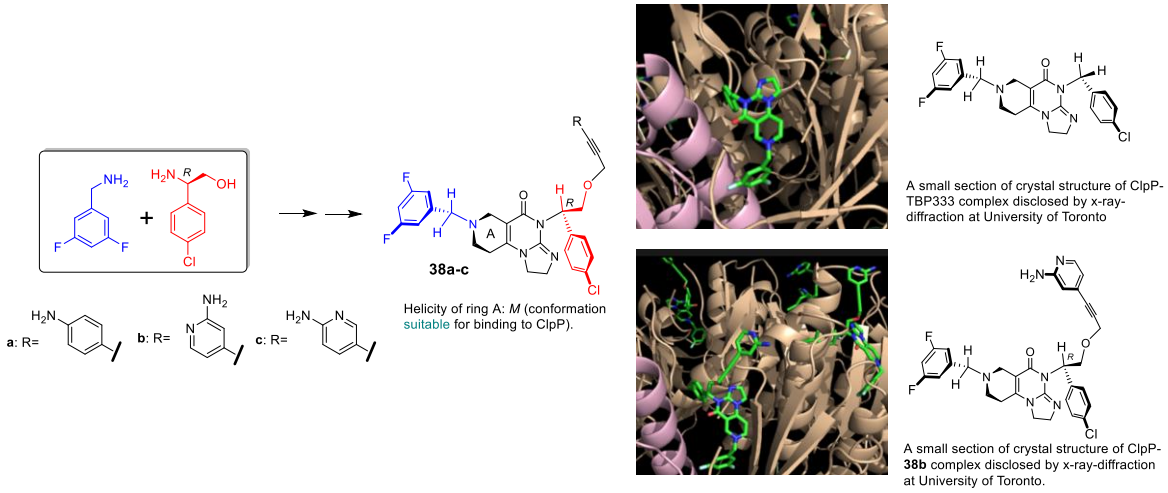

Scheme 6.

In order to assess the benefit derived from the conjugation of the imipridone core with further approved anticancer drugs, an in-depth in vitro study on combination therapy. In this context we reported *in vitro* viability tests performed in two different cell lines (A2058, melanoma; U266, multiple myeloma) to define the potential synergistic activity between the proteasome inhibitor Bortezomib (BOZ) and the TRAIL-inducer ONC201 [11]. The results of endpoint cell viability assays clearly showed synergism between BOZ and ONC201 in A2058 cells after 72 h. The results of the impedance based real time measurement and apoptosis assay have provided further evidence that ONC201 could enhance the bortezomib-induced cell death by sensitizing the cells to BOZ and inducing late apoptosis in combinations. Findings of expression studies have highlighted the role of death receptor proteins (e.g., DR5) and TRAIL protein in the development of synergism between BOZ and ONC201 [11]. Our results support the theory that combination therapy with BOZ + ONC201 may be favourable, and thus these compounds administered together are possible promising candidates for *in vivo* testing in model animals.

Utilizing McMurry reactions of 4,4'-dihydroxybenzophenone with appropriate carbonyl compounds, a series of 4-Hydroxytamoxifen analogues with diverse structures were synthesized. Their cytotoxic activity was evaluated in vitro on four human malignant cell lines (MCF-7, MDA-MB 231, A2058, HT-29). It was found that some of these novel Tamoxifen analogues show marked cytotoxicity in a dose-dependent manner [12]. The relative ROS-generating capability of the synthetized analogues was evaluated by cyclic voltammetry (CV) and DFT modeling studies. The results of cell-viability assays, CV measurements and DFT calculations suggest that the cytotoxicity of the majority of the novel compounds is mainly elicited by their interactions with cellular targets including estrogen receptors rather than triggered by redox processes. However, three novel compounds could be involved in ROS-production and subsequent formation of quinone-methide preventing proliferation and disrupting the redox balance of the treated cells. Among the cell lines studied, HT-29 proved to be the most susceptible to the treatment with compounds having ROS-generating potency [12].

In a separate study it was demonstrated that the added ferrocene moiety in organometallic tamoxifen analogues increases the cytotoxic effect on breast and pancreatic cancer cell lines. The investigated organometallics and tamoxifen are all capable of arresting the cell cycle, but in a concentration-dependent manner, i.e., cell cycle arrest was dominant in concentrations lower than the IC_{50} value of the compounds. Additional research revealed several possible mechanisms that play a role in the cytotoxic effect of the ferrocene-containing tamoxifen derivatives. The dominant pathway they act through depends on the estrogen expression profile of the tumor. On MCF7 cells, where all three isoforms of the ER are expressed, the antagonistic effect on the ER α is predominant. However, GPER1 expression holds back the complete effectivity of tamoxifen, as it increases the

expression levels of several tumor protective proteins. On MDA-MB-231 cells, only ER β is expressed in significant density. The antagonistic effect of tamoxifen on this isoform is clearly dominant on this cell line. On PANC1 cells, only GPER1 expression is detectable. The observed cytotoxic effects elicited by tamoxifen are explainable by non-estrogen receptor-dependent mechanisms, but the GPER1-induced tumor protective pathways interfere with these off-target effects. The ferrocene-linked novel tamoxifen derivatives can counter the GPER1 induced tumor-promoting effects through direct cytotoxicity due to oxidative stress [13].

In order to develop a novel family of hybrids comprising dominant fragment of well-documented amine-based approved therapeutic agent (e.g. Crizotinib or Imatinib) connected to an easily functionalizable small-molecule linker with pending carboxylic group suitable to further functionalisations, we initiated a preliminary synthetic- and structural study on the Mannich reaction of kynureic acid and its modified derivatives (**38**–**40**) having documented relevance in fighting cancer. Using various aldehydes and amine components (**42**–**47**) we have prepared (Scheme 6), characterised and modelled a series of highly functionalized novel kynureic acid derivatives carrying one or two aminoalkyl substituents at different-positions of the hetreocyclic skeleton [14, 15]. By means of DFT calculations it was disclosed that the regioselectivity of the modified Mannich reactions of hydroxykynurenic acids can be rationalised on the basis of the relative acidity of the potential nucleophilic sites as well as the HOMO delocalisation and the local NBO charges in the resulting anions. The spectacular solvent-dependent reactivity of 8-hydroxykynureic acid ester was interpreted by a series of comparative DFT calculations revealing the relative thermodynamics of a polarity-controlled formation of the ion pair involved in the crucial C-C coupling, the iminium-deactivation by the interaction with the solvent used and the polarity-dependent HOMO energy level of the anion component [15]. The novel functionalized kynureic acid derivatives can be considered as the simplified models of some targeted hybrids containing the aforementined and related approved therapeutic agents equipped with propargylamide- or ester residue at C2 position that allow the synthesis of triazole- or alkyne linked chalcones. In this context 6-Hydroxyquinoline and 3-hydroxyisoquinoline as *N*-containing naphthol analogues were also tested in modified Mannich reactions. The highly reagent-and condition-dependent fine-tunable complex reactivity of the substrate was again disclosed and analysed by theoretical modelling studies [16]. The results enable reliable rational design of regioselective functionalizations of the heterocyclic core suitable to be coupled to molecular fragments of approved therapeutic agents.

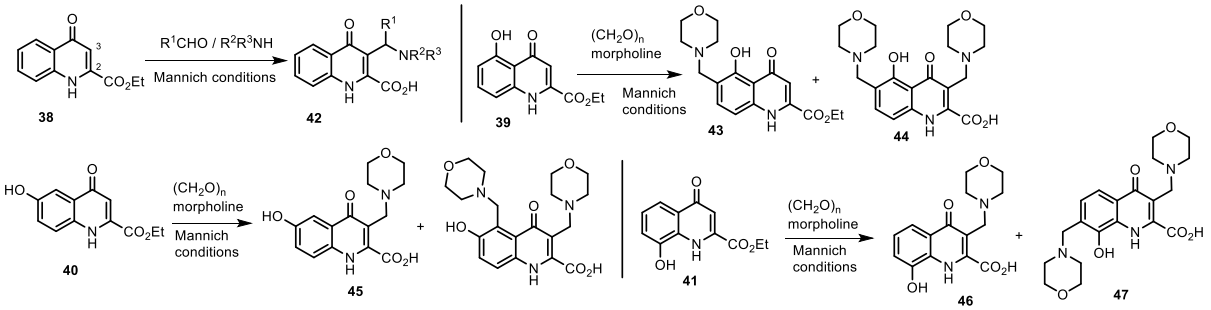

Scheme 6.

In the course of a preliminary synthetic study, two procedures (Scheme 7a and 7b) were elaborated for the construction of the single enantiomers of the first representatives of novel stereoisomer ferroceno-fused pyrrolo[2,1-b]thiazolones and their carboxylates **51**, **52** and **54**, **56**, respectively, of potential interest in a fragment-based design aimed at the identification of such variably functionalisable carboxylic acids with chiral redox-active scaffolds that can be explored in the development of novel enantiomeric potentially bioactive agents. The mechanisms of the multistep annulations proposed on the basis of DFT modelling studies on the relative energetics and control

experiments, accounting for the primary amide formation and diastereoselectivity, were explored in the design and optimization of the synthetic procedures [17].

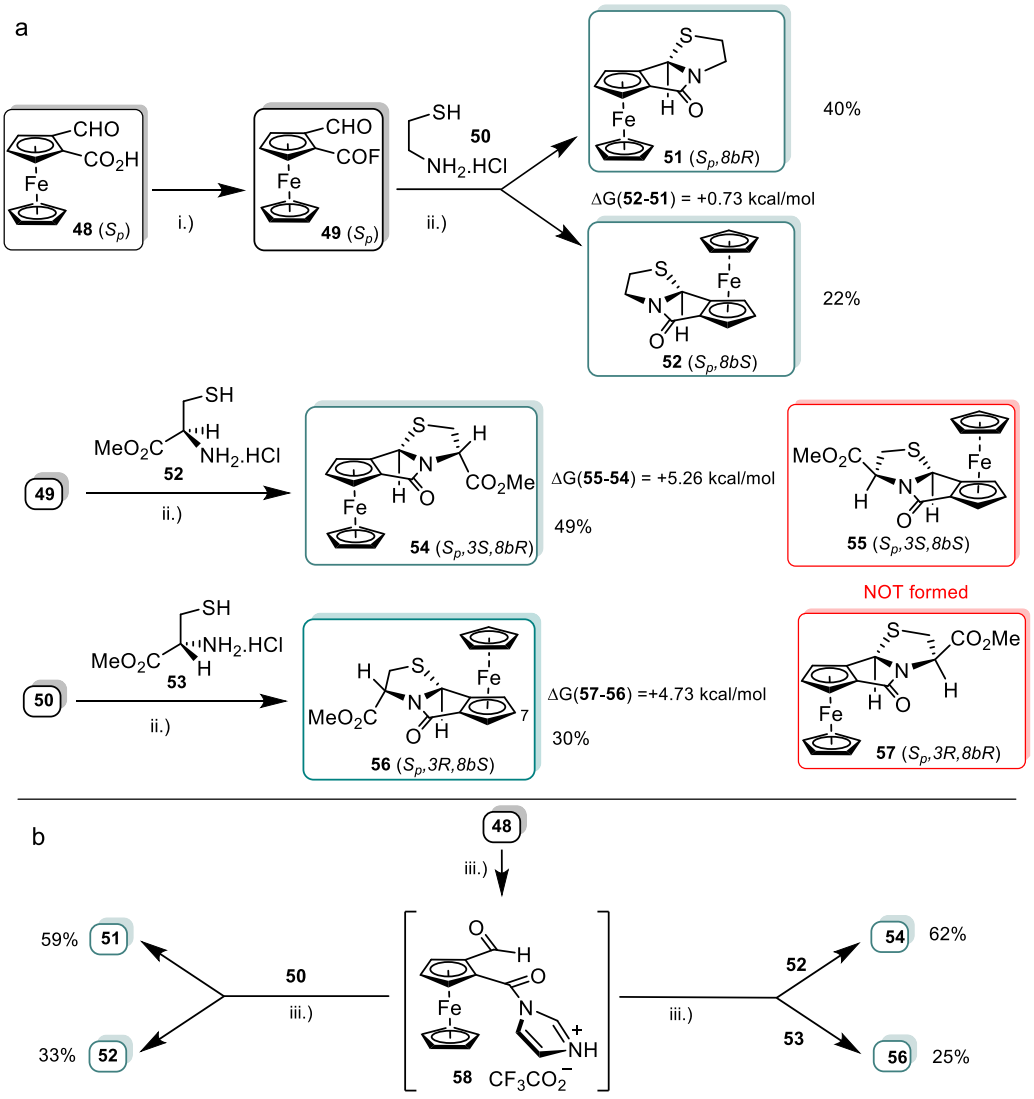

Reaction conditions: i.) cyanuric fluoride, CH_2Cl_2, pyridine, rt., Ar [Ref. 17]; ii.): CH_2Cl_2, pyridine. rt., 2 days, Ar; iii.) CH_2Cl_2, carbonyldiimidazole (CDI), TFA, rt., 2 days, Ar.

Scheme 7.

Publications:

[1] Jernei, T.; Duró, C.; Dembo, A.; Lajkó, E.; Takács, A.; Kőhidai, L.; Schlosser, G.; Csámpai, A. Synthesis, Structure and In Vitro Cytotoxic Activity of Novel Cinchona—Chalcone Hybrids with 1,4-Disubstituted- and 1,5-Disubstituted 1,2,3-Triazole Linkers. *Molecules* **2019**, *24*, 4077. https://doi.org/10.3390/molecules24224077.

[2] Dembo, A.; Jernei, T.; Zupkó, I.; Csámpai, A. Synthesis, Structure and Antiproliferative Activity of Novel C-9-Ferrocenoylamino-substituted Epiquinine—Chalcone Hybrids with 1,4-Disubstituted 1,2,3-Triazole Linkers. The manuscript will be accomplished within one month.

[3] Latif, A.D.; Jernei, T.; Podolski-Renić, A.; Kuo, C.-Y.; Vágvölgyi, M.; Girst, G.; Zupkó, I.; Develi, S.; Ulukaya, E.; Wang, H.-C.; et al. Protoflavone-Chalcone Hybrids Exhibit Enhanced Antitumor Action through Modulating Redox Balance, Depolarizing the Mitochondrial Membrane, and Inhibiting ATR-Dependent Signaling. *Antioxidants* **2020**, *9*, 519. https://doi.org/10.3390/antiox9060519.

[4] Murányi, J.; Duró, C.; Gurbi, B.; Móra, I.; Varga, A.; Németh, K.; Simon, J.; Csala, M.; Csámpai, A. Novel Erlotinib–Chalcone Hybrids Diminish Resistance in Head and Neck Cancer by Inducing Multiple Cell Death Mechanisms. *Int. J. Mol. Sci.* **2023**, *24*, 3456. https://doi.org/10.3390/ijms24043456.

[5] Boulhaoua, M.; Pasinszki, T.; Torvisco, A.; Oláhné Szabó, T., Bősze, Sz.; Csámpai, A. ✉Synthesis, structure and in vitro antiproliferative effects of alkyne-linked 1,2,4-thiadiazole hybrids including erlotinib- and ferrocene-containing derivatives. *RSC Advances*, **2021**, *11*, 46, 28685-28697. doi.org/10.1039/D1RA05095H.

[6] Fodor, K.J.; Hutai, D.; Jernei, T.; Takács, A.; Szász, Z.; Sulyok-Eiler, M.; Harmat, V.; Oláh Szabó, R.; Schlosser, G.; Hudecz, F.; et al. Novel Polycondensed Partly Saturated β-Carbolines Including Ferrocene Derivatives: Synthesis, DFT-Supported Structural Analysis, Mechanism of Some Diastereoselective Transformations and a Preliminary Study of their In Vitro Antiproliferative Effects. *Molecules* **2020**, *25*, 1599. https://doi.org/10.3390/molecules25071599.

[7] Alaoui, N.-E.E.; Boulhaoua, M.; Hutai, D.; Oláh-Szabó, R.; Bősze, S.; Hudecz, F.; Csámpai, A. Synthetic and DFT Modeling Studies on Suzuki–Miyaura Reactions of 4,5-Dibromo-2-methylpyridazin-3(2*H*)-one with Ferrocene Boronates, Accompanied by Hydrodebromination and a Novel Bridge-Forming Annulation In Vitro Cytotoxic Activity of the Ferrocenyl–Pyridazinone Products. *Catalysts* **2022**, *12*, 578. https://doi.org/10.3390/catal12060578.

[8] Csámpai, A.✉; Bárány, P.; Czuczi, T.; Kovács, I.; Adamis, B.; Németh, Zs.; Murányi, J.; Oláhné Szabó, T.; Bősze, Sz.; Mező, G.; Kőhidai, L.; Lajkó, E.; Takács, A.; Láng, O.; Mező, D. Synthesis of novel imipridone derivatives and their evaluation for their anticancer activity. WO2022029459A1. Benyújtás száma: WO2005108388A1

[9] 1. Czuczi, T.; Murányi, J.; Bárány, P.; Móra, I.; Borbély, A.; Csala, M.; Csámpai, A. Synthesis and Antiproliferative Activity of Novel Imipridone–Ferrocene Hybrids with Triazole and Alkyne Linkers. *Pharmaceuticals* **2022**, *15*, 468. https://doi.org/10.3390/ph15040468 (IF: 5.863, Q1)

[10] Czuczi, T.; Móra, I.; Borbély, A.; Csala, M.; Csámpai, A. Aryltriazolylimipridone–Propargylamine Hybrids Capable of Overcoming the Resistance Experienced to ONC201 Treatment: Synthesis, Antiproliferative Evaluation and a Preliminary Mechanistic Study with ClpP Knockout Cells. To be submitted to the *J. Mol. Med*. (IF: 6.427, Q1)

[11]: Takács, A.; Szász, Z.; Kalabay, M.; Bárány, P.; Csámpai, A.; Hegyesi, H.; Láng, O.; Lajkó, E.; Kőhidai, L. The Synergistic Activity of Bortezomib and TIC10 against A2058 Melanoma Cells. *Pharmaceuticals* **2021**, *14*, 820. https://doi.org/10.3390/ph14080820.]

[12] Duró, C.; Jernei, T.; Szekeres, K.J.; Láng, G.G.; Oláh-Szabó, R.; Bősze, S.; Szabó, I.; Hudecz, F.; Csámpai, A. Synthesis and SAR Analysis of Novel 4-Hydroxytamoxifen Analogues Based on Their Cytotoxic Activity and Electron-Donor Character. *Molecules* **2022**, *27*, 6758. https://doi.org/10.3390/molecules27196758].

[13] Kalabay, M.; Szász, Z.; Láng, O.; Lajkó, E.; Pállinger, É.; Duró, C.; Jernei, T.; Csámpai, A.; Takács, A.; Kőhidai, L. Investigation of the Antitumor Effects of Tamoxifen and Its Ferrocene-Linked Derivatives on Pancreatic and Breast Cancer Cell Lines. *Pharmaceuticals* **2022**, *15*, 314. https://doi.org/10.3390/ph15030314.

[14] Lőrinczi, B.; Csámpai, A.; Fülöp, F.; Szatmári, I. Synthesis of New C-3 Substituted Kynurenic Acid Derivatives. *Molecules* **2020**, *25*, 937. https://doi.org/10.3390/molecules25040937

[15] Lőrinczi, B.; Csámpai, A.; Fülöp, F.; Szatmári, I. Synthesis of New C-3 Substituted Kynurenic Acid Derivatives. Synthetic- and DFT modelling studies on regioselective modified Mannich reactions of hydroxy-KYNA derivatives. *RSC Adv*., **2021**, *11*, 543. https://doi.org/10.1039/d0ra08325a.

[16] Csuvik, O.; Barta, P.; Csámpai, A.; Szatmári, I. Fine-Tuned Reactivity of *N*-Containing Naphthol Analogues. *Int. J. Mol. Sci.* **2022**, *23*, 12329. https://doi.org/10.3390/ijms232012329.

[17] Kovács, Z.; Csámpai, A. ✉2,3-Dihydroferroceno[3,4]pyrrolo[2,1-b]thiazol-5(8b)-ones: Synthesis, Structure and DFT Study on the Mechanism of Chemo- and Diastereoslective Annulations of (S_p)-2-Formylferrocenecarbonyl Fluoride and (S_p)-2-Formylferrocenecarboxylic Acid. *Molecules*, **2021**, *26* : 5 Paper: 1420. doi.org/10.3390/molecules26051420.